

# The Effect of Solvent on the Analysis of Secondary Organic Aerosol Using Electrospray Ionization Mass Spectrometry

ADAM P. BATEMAN,<sup>†</sup>  
MAGGIE L. WALSER,<sup>†,‡</sup>  
YURY DESYATERIK,<sup>‡</sup> JULIA LASKIN,<sup>§</sup>  
ALEXANDER LASKIN,<sup>‡</sup> AND  
SERGEY A. NIZKORODOV<sup>\*,†</sup>

Department of Chemistry, University of California, Irvine, Irvine, California 92617-2025, Environmental Molecular Sciences Laboratory, and Chemical and Materials Sciences Division, Pacific Northwest National Laboratory, Richland, Washington 99352

Received May 6, 2008. Revised manuscript received June 29, 2008. Accepted July 29, 2008.

This study examined the effect of solvent on the analysis of organic aerosol extracts using electrospray ionization mass spectrometry (ESI-MS). Secondary organic aerosol (SOA) produced by ozonation of *d*-limonene, as well as several organic molecules with functional groups typical for OA constituents, were extracted in methanol, *d*<sub>3</sub>-methanol, acetonitrile, and *d*<sub>3</sub>-acetonitrile to investigate the extent and relative rates of reactions between analyte and solvent. High resolution ESI-MS showed that reactions of carbonyls with methanol produce significant amounts of hemiacetals and acetals on time scales ranging from several minutes to several days, with the reaction rates increasing in acidified solutions. Carboxylic acid groups were observed to react with methanol resulting in the formation of esters. In contrast, acetonitrile extracts showed no evidence of reactions with analyte molecules, suggesting that acetonitrile is the preferred solvent for SOA extraction. The use of solvent–analyte reactivity as a tool for the improved characterization of functional groups in complex organic mixtures was demonstrated. Direct comparison between mass spectra of the same SOA samples extracted in methanol versus acetonitrile was used to estimate the lower limits for the relative fractions of carbonyls (≥42%) and carboxylic acids (≥55%) in *d*-limonene SOA.

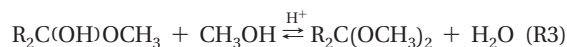
## Introduction

A significant fraction (~50%) of atmospheric particulate matter (PM) contains organic material (1). The organic fraction of PM has been shown to adversely affect human health and to contribute to regional and global climate effects (1). Primary organic aerosol (POA) is emitted directly into the atmosphere by natural and anthropogenic sources. Secondary organic aerosol (SOA) is formed from reactions

between volatile organic compounds and atmospheric oxidants. Both POA and SOA represent a very complex mixture of low volatility, polyfunctional compounds containing alcohol, carbonyl, carboxyl, nitro, and other functionalities (2–7). The high degree of chemical complexity of atmospheric organics has inspired a number of sophisticated methods that are capable of separating and detecting a variety of different analytes in PM samples (8). A common approach involves collection of a sufficient quantity of PM on filters or substrates, extraction of the collected material into suitable solvents, and chromatographic/mass-spectrometric analysis (9–13).

Electrospray ionization mass spectrometry (ESI-MS) offers a number of advantages for the analysis of OA samples (5, 9, 11–16). Coupling ESI to state-of-the-art high resolution MS technologies makes it possible to unambiguously identify multiple components in complex OA extracts based on the accurate mass measurements of individual peaks and their MS/MS fragmentation patterns (12, 17–20). For example, a previous publication from this group described a detailed analysis of *d*-limonene SOA using an LTQ-Orbitrap high resolution mass spectrometer (13). We demonstrated that high-accuracy mass measurements ( $\pm 0.001$  *m/z*) are essential for unambiguous identification of the elemental composition of the hundreds of individual compounds found in SOA extracts. The prevalent ionization mechanisms were deprotonation in the negative ion mode leading to  $[M-H]^-$  ions and complexation with  $Na^+$  in the positive ion mode leading to  $[M+Na]^+$  ions. Data analysis took advantage of Van Krevelen plots (18, 19) to characterize the C:H:O ratios and Kendrick plots (17) to identify homologous families in the reaction products.

Both liquid chromatographic separation and ESI require OA samples to be dissolved in an appropriate solvent. Methanol/water and acetonitrile/water mixtures are the most commonly used solvents in ESI (21). However, one has to keep in mind that polyfunctional compounds found in OA can be reactive with methanol. Specifically, carboxylic acids reacting with methanol may yield esters (R1); carbonyls reacting with methanol may yield hemiacetals (R2) and acetals (R2 and R3) (22).



According to the currently accepted organic nomenclature, ketals are regarded as a subset of acetals; the term “acetal” will be used in reference to both acetals and ketals in the subsequent discussion.

Substantial formation of esterification products was reported in humic acid samples stored in alcohol solvents (23). Because the complexity of OA samples is comparable to that of humic substances (24), we expect similar solvent–analyte reactions to be significant in OA–alcohol extracts as well. Analogous solvent–analyte reactivity has also been reported in the analysis of amoxicillin using ESI-MS in methanol (25). This work examines solvent–analyte reactions of SOA material generated by ozonolysis of monoterpenes and extracted in methanol and acetonitrile for the purposes of direct ESI-MS analysis. In addition, the possibility of using these solvent reactions for qualitative detection of functional groups in OA is explored.

\* Corresponding author phone: 949-824-1262; e-mail: nizkorod@uci.edu.

<sup>†</sup> University of California.

<sup>‡</sup> Environmental Molecular Sciences Laboratory.

<sup>§</sup> Pacific Northwest National Laboratory.

<sup>||</sup> Current address: National Council for Science and the Environment, Washington, DC 20036.

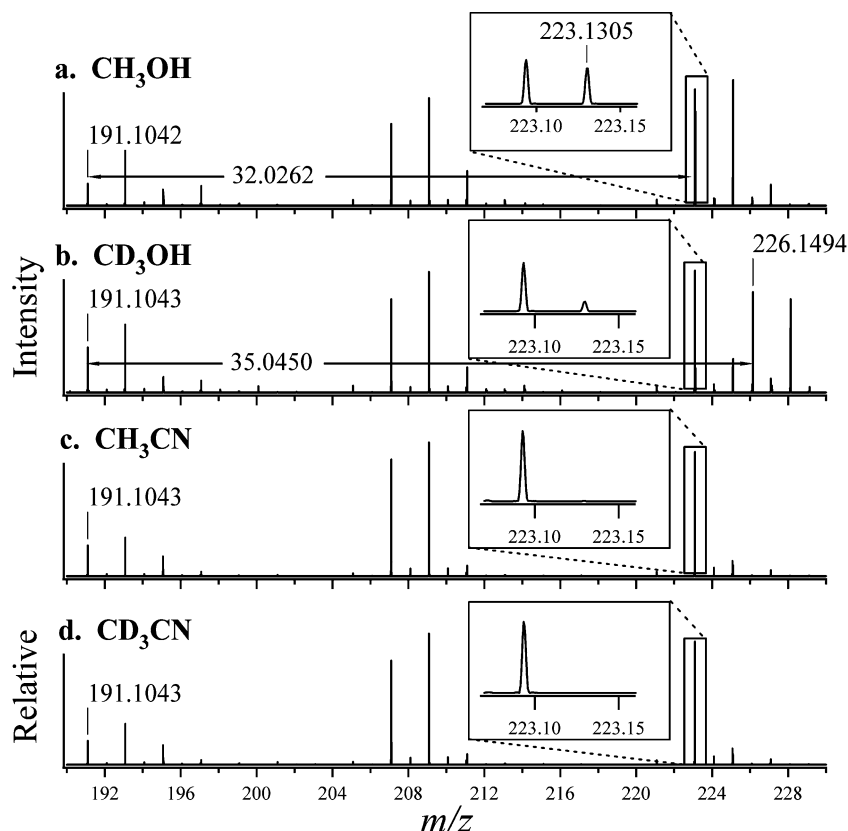


**FIGURE 1.** Sections of ESI positive ion mode mass spectra of the same *d*-limonene SOA sample extracted into four different solvents: (a) methanol; (b)  $d_3$ -methanol; (c) acetonitrile; and (d)  $d_3$ -acetonitrile. Peaks appearing at  $m/z$  223.1305 in methanol and at  $m/z$  226.1494 in  $d_3$ -methanol correspond to hemiacetals of the precursor peak at  $m/z$  191.1043.

## Experimental Method

Laboratory-generated SOA particles were prepared by the ozone-initiated oxidation of *d*-limonene vapor in an inflatable 300 L Teflon reaction chamber as described in ref 13. The particles were collected by pumping the reaction mixture through a glass fiber filter at 30 slpm for ~6 min. The filters were cut into 2–4 equal segments, and each filter segment was separately extracted in 10 mL of a solvent, assisted by sonication, for ~20 min. The solvents included methanol,  $d_3$ -methanol,  $d_4$ -methanol, acetonitrile, and  $d_3$ -acetonitrile. The resulting extracts were filtered through 0.45  $\mu\text{m}$  filters. ESI mass spectra of SOA samples were typically taken minutes to hours after the extraction.

In addition to the SOA samples, ESI mass spectra of three test compounds were investigated (Figure S1 in the Supporting Information). They are referenced by their acronyms throughout this paper. PA refers to *cis*-pinonic acid, a carboxylic acid with an additional ketone group and a major constituent of SOA formed from the oxidation of  $\alpha$ -pinene (10). SS stands for succinic semialdehyde, a carboxylic acid with an additional aldehyde group. DDA refers to 2,5-dioxobicyclo[2.2.2]octane-1,4-dicarboxylic acid, a dicarboxylic acid with two additional ketone groups. Glacial acetic acid was used to acidify the solutions of these test compounds. Commercial sources and purity grades of all chemicals and solvents used in this work are listed in the Supporting Information.

ESI mass spectra of the test compounds were recorded as a function of time since dissolution. Solution concentrations were  $43.5 \pm 5.0 \mu\text{M}$  DDA,  $53.5 \pm 5.0 \mu\text{M}$  PA, and  $186 \pm 10 \mu\text{M}$  SS. The solutions were promptly acidified to achieve acetic acid concentrations of  $16 \pm 2 \mu\text{M}$ ,  $1.6 \pm 0.2 \text{ mM}$ , or  $16 \pm 2 \text{ mM}$ . As all test compounds contain carboxyl groups, the solutions were slightly acidic even without the acetic

acid addition. Solutions were stored in 1.5 mL clear glass vials at room temperature (25 °C) in the dark. At certain time intervals, a ~100  $\mu\text{L}$  aliquot was transferred in a syringe for ESI-MS analysis in both positive and negative modes.

ESI mass spectra were recorded using a Finnigan LTQ (linear ion trap)-Orbitrap hybrid mass spectrometer (Thermo Electron Corporation, Inc.) with a modified ESI source. Samples were injected through a pulled fused silica capillary tip (50  $\mu\text{m}$  i.d.) at a flow rate of 1.00  $\mu\text{L}/\text{min}$ . The system was operated in both positive and negative modes with a resolving power of 60 000 ( $m/\Delta m$  at  $m/z$  400). The  $m/z$  axis was calibrated using standard solutions of caffeine, MRFA, and Ultramark 1621. All  $m/z$  values cited in this paper refer to the experimentally determined calibrated peak positions, which are generally within  $\pm 0.0003 m/z$  of the theoretically predicted masses.

## Results

Figure 1 shows characteristic positive ion mode mass spectra for *d*-limonene SOA extracted into methanol,  $d_3$ -methanol, acetonitrile, and  $d_3$ -acetonitrile. For discussion purposes, only a small portion of each spectrum around  $m/z$  190–230 is displayed. Full spectra recorded in acetonitrile are reported in Walser et al. (13). The mass spectra recorded in acetonitrile and  $d_3$ -acetonitrile are nearly identical. On the contrary, substantial differences exist between mass spectra of the same SOA sample extracted into methanol and acetonitrile, with a number of additional peaks appearing in the methanol-based mass spectra. Furthermore, methanol and  $d_3$ -methanol mass spectra differ from each other in terms of peak positions and relative intensities.

Similar observations were made for the negative ion mode spectra of *d*-limonene SOA; additional peaks appeared in the methanol-based mass spectra, and their isotopic shifts

were consistent with reactions of analytes with one or more methanol molecules. The negative ion mode spectrum of *d*-limonene SOA contained fewer peaks, most of which were also detected in the positive ion mode (13). Because the positive ion mode data set is larger, the following discussion will deal primarily with the positive ion mode mass spectra.

Careful examination of the differences in peak positions reveals that the majority of extra peaks correspond to an addition of one methanol molecule to an existing ion. For example, there is a progression of peaks with a general formula  $C_{10}H_{16}O_nNa^+$ , with  $n$  ranging from 2 to 7, observed in the positive ion mode mass spectra of all solvents (13). Figure 1 includes three members of this progression:  $m/z$  191.1043 ( $n = 2$ ) arising predominantly from limononaldehyde,  $m/z$  207.0992 ( $n = 3$ ), and  $m/z$  223.0942 ( $n = 4$ ). In mass spectra of SOA extracted into methanol, an additional peak is observed at  $m/z$  223.1305, which corresponds to the  $C_{11}H_{20}O_3Na^+$  ion and differs from the limononaldehyde peak by the exact mass of one  $CH_3OH$  molecule. A similar peak is observed at  $m/z$  226.1494 in mass spectra of SOA extracted into  $d_3$ -methanol, which corresponds to the  $C_{11}H_{17}D_3O_3Na^+$  ion and differs from the limononaldehyde peak by one  $CD_3OH$  molecule. A weak peak at  $m/z$  223.1305 also appears in  $d_3$ -methanol based mass spectra, presumably resulting from  $CH_3OH$  residue in  $d_3$ -methanol. Peaks of this nature were also evident in the  $d_4$ -methanol extracts as described in the Supporting Information.

In order to assess the extent of reactions between methanol and various SOA constituents, we compared positive ion mode ESI mass spectra of *d*-limonene SOA samples in  $d_3$ -methanol, methanol, and acetonitrile. Only peaks in the range of  $m/z$  100–500, corresponding to monomeric and dimeric oxidation products (13), above the 0.5% abundance threshold, were selected for analysis. We focused our attention on reactions (R1, R2, and R3) resulting in the following  $m/z$  shifts: 14.0156 ( $+CH_3OH - H_2O$ ) and 17.0345 ( $+CD_3OH - H_2O$ ) for ester formation (R1); 32.0262 ( $+CH_3OH$ ) and 35.0450 ( $+CD_3OH$ ) for hemiacetal formation (R2); and 46.0419 ( $+2CH_3OH - H_2O$ ) and 52.0794 ( $+2CD_3OH - H_2O$ ), for acetal formation (R2R3). It is important to note that interference between different solvent–analyte reactions can introduce ambiguities to the assignment of functional groups, especially for polyfunctional SOA constituents. For example, esterification of a carboxyl group ( $+CH_3OH - H_2O$ ) produces the same mass shift as hemiacetal formation followed by dehydration of an aldehyde. Similarly, acetal formation from a carbonyl ( $+2CH_3OH - H_2O$ ) results in the same mass shift as a concurrent hemiacetal formation and esterification of a molecule that has both carbonyl and carboxyl functional groups. In addition,  $\Delta(m/z)$  values for the  $CH_3OH$  reactions can naturally occur in all solvents because ozonolysis of *d*-limonene generates many homologous families of products (13).

The results of this comparison (described in more detail in Figure S2 in the Supporting Information) clearly demonstrate that mass spectra recorded in  $CD_3OH$  provide the most information about the extent of solvent–analyte reactions. Positive ion mode  $d_3$ -methanol-based spectra contained over 200 peaks at even  $m/z$  values attributable to the solvent–analyte reaction products. In most cases, these peaks could be clearly distinguished from the isobaric  $^{13}C$  containing ions, based on the relative abundance and exact  $m/z$  values. Specifically, 189 pairs of peaks were separated by the exact mass of  $d_3$ -methanol, representing hemiacetal formation. In addition, there were 198 pairs of peaks corresponding to the formation of esters, and 41 pairs corresponding to the formation of acetals. In more than 100 instances, the same products were formed by more than one reaction (R1, R2, and R3) because of the simultaneous

presence of both carbonyl and carboxyl functional groups in many SOA constituents.

Figure 2 is a graphical representation of the extent of solvent–analyte reactions in SOA extracts. It compares the positive ion mode mass spectrum of *d*-limonene SOA recorded in acetonitrile with mass spectra of the same SOA sample recorded in methanol and  $d_3$ -methanol. The acetonitrile-based mass spectra (top) contains all peaks with  $>0.5\%$  relative intensity, including those from  $^{13}C$  containing ions. In contrast, the methanol- and  $d_3$ -methanol-based spectra (bottom) include only peaks corresponding to compounds capable of forming hemiacetals. Approximately 39% of *d*-limonene oxidation products in the monomeric range and 47% in the dimeric range are capable of adding one methanol molecule to form a hemiacetal. We stress that it is not just the smallest peaks that are affected by the methanol–analyte reactions. For example, if we limit the discussion only to peaks with relative abundance greater than 2% of the base peak (instead of 0.5%), the fraction of compounds capable of forming hemiacetals increases to 55% in the monomeric range and to 63% in the dimeric range.

To examine reactions occurring in methanol under more controlled conditions, we compared ESI mass spectra of the test compounds shown in Figure S1 using  $d_3$ -methanol, methanol, and acetonitrile as electrospray solvents. All test chemicals contain a carboxylic acid group, and their mass spectra in acetonitrile are dominated by the  $[M+Na]^+$  and  $[M-H]^-$  peaks in the positive and negative ion modes, respectively. In addition, these test compounds have one or two carbonyl groups, leading to the appearance of the corresponding ester and acetal peaks in the  $d_3$ -methanol and methanol spectra.

Sample measurements of product peak intensities as a function of the storage time are presented in Figure 3, wherein all intensities are normalized to the corresponding precursor peaks. The hemiacetal product peaks had a comparatively weak dependence on storage time and solution acidity. For example, Figure 3a and Figure 3b show the abundances of hemiacetals of SS and DDA, respectively. In both cases, the relative abundance of the hemiacetal started at a high initial value of  $\sim 5$  and  $\sim 0.6$  for SS and DDA, respectively, and remained constant with time within the experimental uncertainty. These hemiacetals presumably attained an equilibrium with their precursor carbonyls *before* the first mass spectrum was taken (in less than  $\sim 5$  min), and this equilibrium was then slowly shifted by the much slower acetal formation. We conclude that solvent–analyte reactions can result in large peaks appearing in the ESI mass spectra immediately after the sample preparation.

The intensity of the ester product peaks grew considerably more slowly with time. For example, all DDA solutions reached the ester  $\leftrightarrow$  DDA equilibrium in less than 24 h with no apparent dependence on the acetic acid concentration (Figure 3c). On the contrary, the PA solutions did not attain the ester  $\leftrightarrow$  PA equilibrium even after 90 h of storage, although the extent of the reaction noticeably increased with acidity (Figure 3d). The normalized abundance was larger for the DDA ester compared to that for the PA ester, presumably due to the presence of two carboxylic groups in DDA.

The acetal product peaks slowly increased in their relative abundance as a function of both time and solution acidity. For example, the relative abundance of the PA acetal (Figure 3e) started at a very low initial value, and reached a steady state corresponding to the acetal  $\leftrightarrow$  PA equilibrium after about one day of storage in solutions acidified with 16 mM and 1.6 mM acetic acid. Solutions containing 16  $\mu M$  or no acetic acid did not reach equilibrium even after one week of storage. The relative abundance of the SS acetal (Figure 3f) similarly increased with time and with solution acidity. However, the

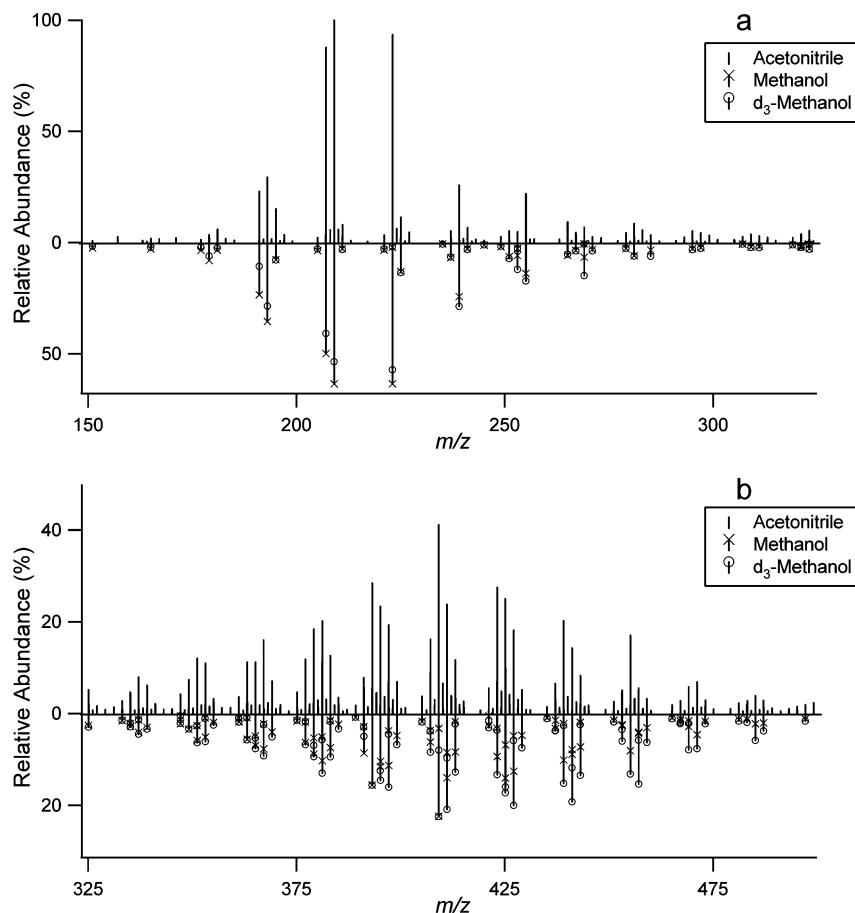


**FIGURE 2.** Graphical representation of the fraction of SOA compounds capable of forming hemiacetal products. The monomer range (a) and dimer range (b) are displayed separately for clarity. The full *d*-limonene SOA positive ion mode mass spectrum recorded in acetonitrile is given in the positive portions of the graphs. The negative portions display mass spectra recorded in methanol and *d*<sub>3</sub>-methanol, and include only peaks corresponding to compounds capable of forming hemiacetals.

system was far from the acetal ↔ SS equilibrium even after one week of storage in the presence of 16 mM acetic acid.

## Discussion

Drastic changes in the SOA mass spectrum resulting from isotopic substitution in the solvent molecules (methanol → *d*<sub>3</sub>-methanol) clearly demonstrate that many SOA constituents undergo chemical reactions with methanol during extraction, storage, and possibly during the electrospray process. The reaction equilibria (R1, R2, and R3) generally favor the initial reactants but can be pushed toward the products with excess methanol, i.e., under typical conditions of extraction of a small quantity of organic material by a large volume of solvent. In addition, excess methanol can replace all –OR groups in various esters present in SOA sample with –OCH<sub>3</sub> groups introducing additional artifacts to the mass spectra.

As opposed to the methanol case, isotopic substitution of acetonitrile for *d*<sub>3</sub>-acetonitrile has nearly no effect on the appearance of ESI mass spectra of SOA samples. Acetonitrile can undergo addition reactions with certain alcohols in the presence of concentrated acids (26). In the presence of strong bases, acetonitrile can be deprotonated to form the cyanomethide ion, which is reactive toward carbonyls (27) and alcohols (28). The laboratory-generated OA extracts as well as extracts of field PM samples are expected to be neutral or weakly acidic (29). Reactions of carbonyls and alcohols with acetonitrile are very unlikely under such mild conditions.

Formation of esters, hemiacetals, and acetals is well-known to be acid-catalyzed (22). Therefore the effect of

increasing acidity should lead to the faster appearance of reaction products in the mass spectra. This prediction is consistent with the observed time dependence of solvent reactions with test species SS, PA, and DDA (Figure 3). As expected, the acidity affects the rate but not the extent of the reaction: given enough time the same final equilibrium state is attained. The observed reduction of the hemiacetal peaks with the solution acidity (e.g., Figure 3a) can be explained by assuming fast carbonyl/hemiacetal equilibrium, followed by much slower hemiacetal/acetal equilibrium. As the solution acidity increases, the latter equilibrium is attained faster, leading to the relative increase in the acetal peak at the expense of the hemiacetal and analyte peaks.

Table S1 in the Supporting Information lists the relative abundance of the methanol–analyte reaction peaks from each test solution after 24 h of storage. The methanol–analyte reaction peak abundances are normalized to the abundances of the [M+Na]<sup>+</sup> and [M–H]<sup>–</sup> precursor ions in the positive and negative ion mode, respectively. The relative abundance of product peaks is generally quite small, often smaller than a fraction of a percent. For example, all product peaks for PA are <0.3% of the precursor acid peak. However, relative abundances of the SS product peaks are quite significant. The SS hemiacetal and ester peaks are, in fact, both larger than the SS peak in the positive ion mode. The hemiacetal and ester of DDA are also fairly abundant. The observed trend in reactivity toward methanol, SS > DDA > PA, is consistent with the higher reactivity of aldehydes versus ketones toward methanol due to both steric and electronic factors (22). In addition, large substituent groups in carbonyls

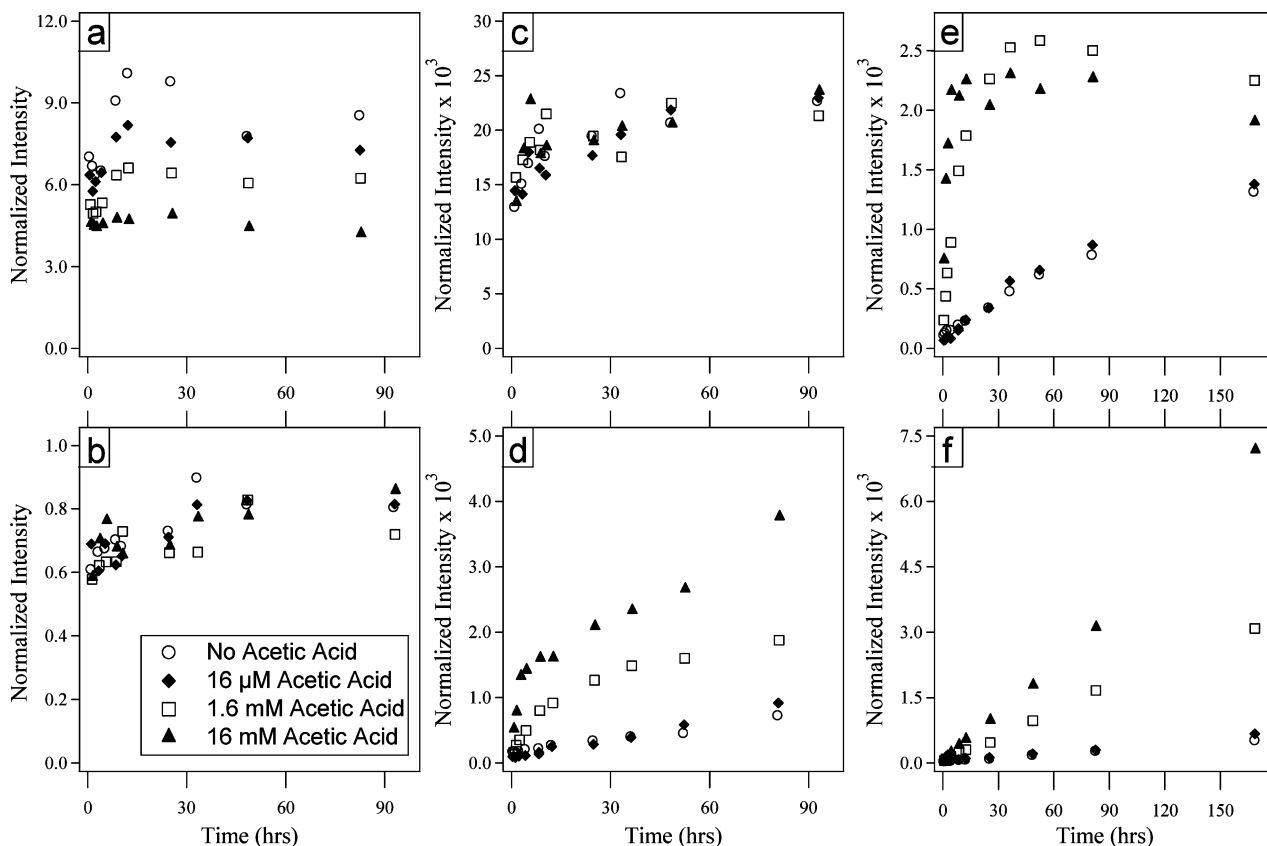


**FIGURE 3.** Representative data for the time dependent growth of products in reactions of test compounds with methanol: (a) hemiacetal of SS; (b) hemiacetal of DDA; (c) ester of DDA; (d) ester of PA; (e) acetal of PA; and (f) acetal of SS. All product intensities are measured in the positive ion mode and normalized to the corresponding precursor ion.

**TABLE 1.** Observed Reactivity of OA Components with  $d_3$ -Methanol<sup>a</sup>

New peak at $\Delta m/z$ in $d_3$ -methanol	product	functional group	observed fraction in $d$ -limonene SOA (%)
+35.0450	hemiacetal	carbonyl carboxylic	~42
+17.0345	ester <sup>b</sup>	acid	~55
+52.0794	acetal <sup>c</sup>	carbonyl	~13

<sup>a</sup> The last column provides approximate lower limits for the percentages of carbonyls and carboxyls in  $d$ -limonene SOA. <sup>b</sup> Can also result from hemiacetal formation followed by dehydration. <sup>c</sup> Can also result from hemiacetal formation followed by esterification.

tend to shift the equilibria (R1, R2, and R3) toward the initial reactants, i.e., away from ester, hemiacetal, and acetal formation (30).

Table 1 shows how a direct comparison of mass spectra of the same sample dissolved in acetonitrile and  $d_3$ -methanol can be used to detect carbonyl and carboxyl groups in SOA constituents. Isotopically labeled methanol should be used for such a comparison because of the natural occurrence of  $\text{CH}_2$ - and  $\text{H}_2\text{O}$ - homologous series in SOA samples (12, 13). Direct counting of peaks in  $d$ -limonene SOA positive ion mode mass spectrum between  $m/z$  150–500 and above the 2% abundance threshold suggest that at least 42 and 55% of detectable SOA constituents contain carbonyl and carboxylic acid groups, respectively. This may appear unrealistically low given the extent of  $d$ -limonene oxidation reported in ref 13, with the O:C ratio approaching ~0.5. However, this peak-counting approach is expected to provide only a lower limit for the fraction of carbonyls and carboxyls in the sample

because not every OA constituent is sufficiently reactive with methanol to produce significant product peaks in the ESI mass spectrum. Furthermore, the polyfunctional nature of SOA constituents could result in the simultaneous derivatization of multiple functional groups within the same molecule, which cannot be assigned using this simple peak counting procedure. The remaining oxygen required to achieve the high O:C ratio observed in ref 13 most likely resides in hydroxyl, ether, and peroxy functional groups in SOA constituents, which do not readily react with methanol.

The potential utility of solvent-analyte reactivity as a tool for interpretation of ESI mass spectra of SOA samples is further illustrated in Table S2 in the Supporting Information. Table S2 lists the intensities of the five largest peaks in the  $d$ -limonene SOA positive ion mass spectrum in acetonitrile and classifies them as either aldehydes or ketones, based on the peak intensity of the hemiacetal compared to that of the precursor carbonyl. Table S2 clearly demonstrates that all major SOA constituents listed in the table contain a carbonyl group. This is consistent with the known mechanism of gas-phase ozonolysis of alkenes, which generates carbonyls in high yields by splitting unstable primary ozonides, and carboxylic acids by isomerization of carbonyl oxides (13). Table S2 also shows that the peaks corresponding to the reactions between SOA constituents and methanol have appreciable intensities. Indeed, the most abundant peaks observed in the positive ion mode ESI mass spectra of  $d$ -limonene in methanol and  $d_3$ -methanol correspond to hemiacetals. We conclude that solvent-analyte reactions occur to a significant extent in methanol extracts and should be taken into serious consideration in the analysis of organic aerosol samples by ESI-MS.

## Acknowledgments

The UCI researchers acknowledge support provided by U.S. National Science Foundation through the EMSI program, CHE-0431312, and Atmospheric Chemistry program, ATM-0509248. The Pacific Northwest National Laboratory (PNNL) research group acknowledges support from the Chemical Sciences Division, of the Office of Basic Energy Sciences, Department of Energy, and the Atmospheric Science Program of the Office of Biological and Environmental Research, Department of Energy. This work was performed at the W. R. Wiley Environmental Molecular Sciences Laboratory, a national scientific user facility sponsored by the Office of Biological and Environmental Research and located at PNNL. PNNL is operated for the U.S. Department of Energy by Battelle Memorial Institute under contract no. DE-AC06-76RL0 1830. A.P.B. acknowledges sponsorship provided by the 2007 Summer Research Institute organized at PNNL.

## Supporting Information Available

Information on purity and sources of chemicals used; Figure S1 with structures of test chemicals; Figure S2 with frequencies of occurrence of  $m/z$  differences corresponding to reactions (R1, R2, and R3) in the SOA mass spectra; Table S1 with relative ion abundances in mass spectra of test chemicals; Table S2 with intensities of 5 major peaks in SOA mass spectra in different solvents, and additional discussion. This material is available free of charge via the Internet at <http://pubs.acs.org>.

## Literature Cited

- (1) Kanakidou, M.; Seinfeld, J. H.; Pandis, S. N.; Barnes, I.; Dentener, F. J.; Facchini, M. C.; Van Dingenen, R.; Ervens, B.; Nenes, A.; Nielsen, C. J.; Swietlicki, E.; Putaud, J. P.; Balkanski, Y.; Fuzzi, S.; Horth, J.; Moortgat, G. K.; Winterhalter, R.; Myhre, C. E. L.; Tsigaridis, K.; Vignati, E.; Stephanou, E. G.; Wilson, J. Organic aerosol and global climate modelling: a review. *Atm. Chem. Phys.* **2005**, *5*, 1053–1123.
- (2) Hildemann, L. M.; Markowski, G. R.; Cass, G. R. Chemical composition of emissions from urban sources of fine organic aerosol. *Environ. Sci. Technol.* **1991**, *25*, 744–759.
- (3) Rogge, W. F.; Mazurek, M. A.; Hildemann, L. M.; Cass, G. R.; Simoneit, B. R. T. Quantification of urban organic aerosols at a molecular level: identification, abundance and seasonal variation. *Atmos. Environ.* **1993**, *27A*, 1309–1330.
- (4) Nolte, C. G.; Schauer, J. J.; Cass, G. R.; Simoneit, B. R. T. Highly polar organic compounds present in meat smoke. *Environ. Sci. Technol.* **1999**, *33*, 3313–3316.
- (5) Tolocka, M. P.; Jang, M.; Ginter, J. M.; Cox, F. J.; Kamens, R. M.; Johnston, M. V. Formation of oligomers in secondary organic aerosol. *Environ. Sci. Technol.* **2004**, *38*, 1428–1434.
- (6) Surratt, J. D.; Kroll, J. H.; Kleindienst, T. E.; Edney, E. O.; Claeys, M.; Sorooshian, A.; Ng, N. L.; Offenberg, J. H.; Lewandowski, M.; Jaoui, M.; Flagan, R. C.; Seinfeld, J. H. Evidence for organosulfates in secondary organic aerosol. *Environ. Sci. Technol.* **2007**, *41*, 517–527.
- (7) Iinuma, Y.; Mueller, C.; Boege, O.; Gnauk, T.; Herrmann, H. The formation of organic sulfate esters in the limonene ozonolysis secondary organic aerosol (SOA) under acidic conditions. *Atmos. Environ.* **2007**, *41*, 5571–5583.
- (8) Sipin, M. F.; Guazzotti, S. A.; Prather, K. A. Recent advances and some remaining challenges in analytical chemistry of the atmosphere. *Anal. Chem.* **2003**, *75*, 2929–2940.
- (9) Glasius, M.; Duane, M.; Larsen, B. R. Determination of polar terpene oxidation products in aerosols by liquid chromatography-ion trap mass spectrometry. *J. Chromatogr., A* **1999**, *833*, 121–135.
- (10) Jang, M.; Kamens, R. M. Newly characterized products and composition of secondary aerosols from the reaction of  $\alpha$ -pinene with ozone. *Atmos. Environ.* **1999**, *33*, 459–474.
- (11) Szmigielski, R.; Surratt, J. D.; Vermeylen, R.; Szmigielska, K.; Kroll, J. H.; Ng, N. L.; Murphy, S. M.; Sorooshian, A.; Seinfeld, J. H.; Claeys, M. Characterization of 2-methylglyceric acid oligomers in secondary organic aerosol formed from the photooxidation of isoprene using trimethylsilylation and gas chromatography/ion trap mass spectrometry. *J. Mass Spectrom.* **2007**, *42*, 101–116.
- (12) Reinhardt, A.; Emmenegger, C.; Gerrits, B.; Panse, C.; Dommen, J.; Baltensperger, U.; Zenobi, R.; Kalberer, M. Ultrahigh mass resolution and accurate mass measurements as a tool to characterize oligomers in secondary organic aerosols. *Anal. Chem.* **2007**, *79*, 4074–4082.
- (13) Walser, M. L.; Dessiaterik, Y.; Laskin, J.; Laskin, A.; Nizkorodov, S. A. High-resolution mass spectrometric analysis of secondary organic aerosol produced by ozonation of limonene. *Phys. Chem. Chem. Phys.* **2008**, *10*, 1009–1022.
- (14) Surratt, J. D.; Murphy, S. M.; Kroll, J. H.; Ng, N. L.; Hildebrandt, L.; Sorooshian, A.; Szmigielski, R.; Vermeylen, R.; Maenhaut, W.; Claeys, M.; Flagan, R. C.; Seinfeld, J. H. Chemical composition of secondary organic aerosol formed from the photooxidation of isoprene. *J. Phys. Chem. A* **2006**, *110*, 9665–9690.
- (15) Iinuma, Y.; Mueller, C.; Berndt, T.; Boege, O.; Claeys, M.; Herrmann, H. Evidence for the existence of organosulfates from  $\beta$ -pinene ozonolysis in ambient secondary organic aerosol. *Environ. Sci. Technol.* **2007**, *41*, 6678–6683.
- (16) Hamilton, J. F.; Lewis, A. C.; Carey, T. J.; Wenger, J. C. Characterization of polar compounds and oligomers in secondary organic aerosol using liquid chromatography coupled to mass spectrometry. *Anal. Chem.* **2008**, *80*, 474–480.
- (17) Hughey, C. A.; Hendrickson, C. L.; Rodgers, R. P.; Marshall, A. G.; Qian, K. Kendrick mass defect spectrum: a compact visual analysis for ultrahigh-resolution broadband mass spectra. *Anal. Chem.* **2001**, *73*, 4676–4681.
- (18) Wu, Z.; Rodgers, R. P.; Marshall, A. G. Two- and three-dimensional van Krevelen diagrams: a graphical analysis complementary to the Kendrick mass plot for sorting elemental compositions of complex organic mixtures based on ultrahigh-resolution broadband Fourier transform ion cyclotron resonance mass measurements. *Anal. Chem.* **2004**, *76*, 2511–2516.
- (19) Kim, S.; Kramer, R. W.; Hatcher, P. G. Graphical method for analysis of ultrahigh-resolution broadband mass spectra of natural organic matter, the van Krevelen diagram. *Anal. Chem.* **2003**, *75*, 5336–5344.
- (20) Warscheid, B.; Hoffmann, T. Structural elucidation of monoterpene oxidation products by ion trap fragmentation using on-line atmospheric pressure chemical ionization mass spectrometry in the negative ion mode. *Rap. Comm. Mass Spectrom.* **2001**, *15*, 2259–2272.
- (21) Cech, N. B.; Enke, C. G. Practical implications of some recent studies in electrospray ionization fundamentals. *Mass Spectrom. Rev.* **2001**, *20*, 362–387.
- (22) Solomons, T. W. G.; Fryhle, C. B. *Organic Chemistry*; 7th ed.; John Wiley and Sons: New York, 2002.
- (23) McIntyre, C.; McRae, C. Proposed guidelines for sample preparation and ESI-MS analysis of humic substances to avoid self-esterification. *Org. Geochem.* **2005**, *36*, 543–553.
- (24) Graber, E. R.; Rudich, Y. Atmospheric HULIS: How humic-like are they? A comprehensive and critical review. *Atm. Chem. Phys.* **2006**, *6*, 729–753.
- (25) Grujic, S.; Vasiljevic, T.; Lausevic, M.; Ast, T. Study on the formation of an amoxicillin adduct with methanol using electrospray ion trap tandem mass spectrometry. *Rapid Commun. Mass Spectrom.* **2008**, *22*, 67–74.
- (26) Parris, C. L.; Christenson, R. M. *N*-alkylation of nitriles with benzyl alcohol, related alcohols, and glycols. *J. Org. Chem.* **1960**, *25*, 331–334.
- (27) DiBiase, S. A.; Lipisko, B. A.; Haag, A.; Wolak, R. A.; Gokel, G. W. Direct synthesis of  $\alpha,\beta$ -unsaturated nitriles from acetonitrile and carbonyl compounds: survey, crown effects, and experimental conditions. *J. Org. Chem.* **1979**, *44*, 4640–4649.
- (28) Roger, R.; Neilson, D. G. The chemistry of imidates. *Chem. Rev.* **1961**, *61*, 179–211.
- (29) Gao, S.; Surratt, J. D.; Knipping, E. M.; Edgerton, E. S.; Shahgholi, M.; Seinfeld, J. H. Characterization of polar organic components in fine aerosols in the southeastern United States: Identity, origin, and evolution. *J. Geophys. Res.* **2006**, *111*D14314, DOI: 10.1029/2005JD006601.
- (30) Roberts, J. D.; Caserio, M. C. *Basic Principles of Organic Chemistry*; 2nd ed.; W. A. Benjamin, Inc.: Menlo Park, CA, 1977.

ES801226W